Journal of Power Sources 188 (2009) 552–557

Contents lists available at ScienceDirect

Journal of Power Sources

journal homepage: www.elsevier.com/locate/jpowsour

Ternary Sn–Sb–Co alloy film as new negative electrode for lithium-ion cells

T. Tabuchi [a,b,*], N. Hochgatterer [a], Z. Ogumi [b], M. Winter [a]

[a] Institute for Chemical Technology of Inorganic Materials, Technical University of Graz, Stremayrgasse 16, Graz 8010, Austria
[b] Graduate School of Engineering, Kyoto University, Kyotodaigaku-katsura, Nishikyo-ku, Kyoto 615-8510, Japan

ARTICLE INFO

Article history:
Received 10 June 2008
Received in revised form 5 November 2008
Accepted 28 November 2008
Available online 6 December 2008

Keywords:
Sn alloy
Negative electrode
Film
Electroplating

ABSTRACT

Ternary Sn–Sb–Co alloy film was successfully prepared by the co-electroplating method using an aqueous solution bath containing $SnCl_2{\cdot}2H_2O$, $CoCl_2$, $SbCl_3$, $Na_2C_4H_4O_6{\cdot}2H_2O$, $K_3C_6H_5O_7{\cdot}H_2O$, and gelatine. The alloy composition was found to be mainly controllable by the amount of $Na_2C_4H_4O_6{\cdot}2H_2O$ and $SbCl_3$ in the plating bath. The Sn–Sb–Co film electrode with a composition of 75.4% Sn, 6.5% Sb, and 18.1% Co gave an initial discharge capacity of 380 mAh g^{-1}. The capacity gradually increased from the 1st to the 10th cycle and was then stabilized at a larger value of 580 mAh g^{-1}. Furthermore, the electrode was found to give better cycle performance compared to binary Sn–Co and Sn–Sb alloys.

1. Introduction

Commerce-based lithium-ion cells have been developed for practical use mainly for cellular phones and notebook computers by using a carbon negative electrode, which has a theoretical capacity of 372 mAh g^{-1}. However, the enlargement of energy density has been limited due to the small capacity of the conventional electrode. Therefore, Sn-based alloy has been extensively studied for the reason that the large theoretical capacity of 991 mAh g^{-1} is more attractive than carbon materials [1–3]. Nevertheless, there still remains the problem as regards the capacity decay with cycling. This is because the lack of electro-conductivity is mainly caused by the significant volume changes of the electrode during charging and discharging. Therefore, composite alloys with other metal elements such as Sb [1,4–12] and Co [13–17] have been proposed to overcome this problem. There are mainly two composite types of alloy to improve the cycleability. In one scenario, one metal element of the alloys is first displaced with Li as Li insertion proceeds, resulting in the formation of pure metal, which acts to buffer volume changes. After this reaction, Li is further inserted in the pure metal [9]:

$$(x+y)\mathrm{Li} + \mathrm{MM}'_z \Leftrightarrow y\mathrm{Li} + \mathrm{Li}_x\mathrm{M} + z\mathrm{M}'$$

$$y\mathrm{Li} + \mathrm{Li}_x\mathrm{M} + z\mathrm{M}' \Leftrightarrow \mathrm{Li}_x\mathrm{M} + z\mathrm{Li}_{y/z}\mathrm{M}'$$

Sn–Sb alloy is an example of this type where the elements of Sn and Sb react with Li one after another. The non-reacting element or already Li-inserted alloy works as a matrix to reduce the volume changes of the other Li-insertion reaction.

In the second scenario, one metal element of the alloys is displaced with Li while the other, which acts to buffer volume changes, is unable to react with Li [9]:

$$x\mathrm{Li} + \mathrm{MM}'_y \rightarrow \mathrm{Li}_x\mathrm{M} + y\mathrm{M}'$$

$$\mathrm{Li}_x\mathrm{M} + y\mathrm{M}' \Leftrightarrow x\mathrm{Li} + \mathrm{M} + y\mathrm{M}'$$

Sn–Co alloy is an example of this type, which has an inactive Co matrix. Thus, it is important that the composition and role of elements are discussed in order to improve cycle performance of such a Sn-based alloy electrode. In addition, there has been little study done concerning the preparation of ternary alloy film by the electroplating method.

In this work, an electroplating condition was first investigated to prepare the ternary Sn–Sb–Co alloy films in addition to the binary Sn–Co and Sn–Sb materials. With respect to the preparation of Sn–Sb–Co alloy film by means of the electroplating method, the standard electrode potentials of Sn (−0.136 V), Sb (+0.212 V), and Co (−0.277 V) are quite different so that the ternary alloy is unable to form without their complex reagents, which act to reduce the difference. Therefore, new plating bath conditions were investigated in order to obtain a homogeneous Sn–Sb–Co alloy film. Furthermore, the effect of composition on electrochemical properties was then studied to improve the cycle performance of Sn-based alloy electrodes.

* Corresponding author at: Graduate School of Engineering, Kyoto University, Kyotodaigaku-katsura, Nishikyo-ku, Kyoto 615-8510, Japan. Tel.: +81 75 383 2488; fax: +81 75 383 2488.
E-mail address: toru.tabuchi@jp.gs-yuasa.com (T. Tabuchi).

0378-7753/$ – see front matter © 2008 Elsevier B.V. All rights reserved.
doi:10.1016/j.jpowsour.2008.11.116

Table 1
Plating bath conditions for binary Sn–Co alloy film.

	(a)	(b)	(c)	(d)	(e)	(f)	(g)	(h)	(i)
$SnCl_2{\cdot}2H_2O$	5.8	5.8	5.8	5.8	5.8	5.8	5.8	5.8	5.8
$CoCl_2$	5.8	8.7	11.6	17.3	17.3	17.3	173	173	17.3
$Na_2C_4H_4O_6{\cdot}2H_2O$	150.0	150.0	150.0	150.0	250.0	350.0	350.0	350.0	350.0
$K_3C_6H_5O_7{\cdot}H_2O$	20.0	20.0	20.0	20.0	20.0	20.0	40.0	80.0	160.0
Gelatine	0.4	0.4	0.4	0.4	0.4	0.4	0.4	0.4	0.4

$g\,L^{-1}$.

Table 2
Plating bath conditions for ternary Sn–Sb–Co alloy film.

	(j)	(k)	(l)	(m)
$SnCl_2{\cdot}2H_2O$	5.8	5.3	5.8	5.8
$SbCl_3$	09	1.8	2.7	3.6
$CoCl_2$	17.3	17.3	17.3	17.3
$Na_2C_4H_4O_6{\cdot}2H_2O$	150.0	150.0	150.0	150.0
$K_3C_6H_5O_7{\cdot}H_2O$	20.0	20.0	20.0	20.0
Gelatine	0.4	0.4	0.4	0.4

$g\,L^{-1}$.

2. Experimental

Sn–Sb–Co and Sn–Co alloy films were prepared on the rough surface of Cu substrate by the co-electroplating method. The Cu substrate was treated with 30% H_2SO_4 aqueous solution for 60 s before the electroplating. $SnCl_2{\cdot}2H_2O$, $CoCl_2$, and $SbCl_3$ were used as metal resource reagents. $Na_2C_4H_4O_6{\cdot}2H_2O$ and $K_3C_6H_5O_7{\cdot}H_2O$ were used as complex reagents. Gelatine was used as a viscosity control reagent to form films with homogeneous surfaces. The detailed information of plating bath is summarized in Tables 1 and 2. Sn–Sb alloy electrode was also prepared on the rough Cu substrate for a comparison. The plating bath was an aqueous solution composed of 30.0 $g\,L^{-1}$ $SnCl_2{\cdot}2H_2O$, 1.8 $g\,L^{-1}$ $SbCl_3$, 115 $g\,L^{-1}$ $Na_4P_2O_7{\cdot}10H_2O$, 7.0 $g\,L^{-1}$ tartaric acid, and 0.4 $g\,L^{-1}$ gelatine [8]. In order to prepare all alloy films, the electroplating was carried out at a current density of 2.5 $mA\,cm^{-2}$ for 27 min at 44 °C without stirring to be a thickness of 2–3 μm. Pt and Sn counter electrodes were used for preparing Sn–Sb–Co and Sn–Sb alloy films, respectively. Both Sn and Pt counter electrodes were used for preparing Sn–Co alloy film in order to investigate each influence on the composition.

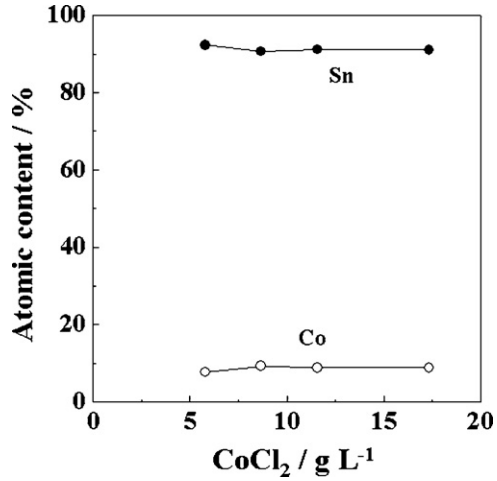

Fig. 2. Change in composition of Sn–Co alloy film as a function of $CoCl_2$ content in the plating bath.

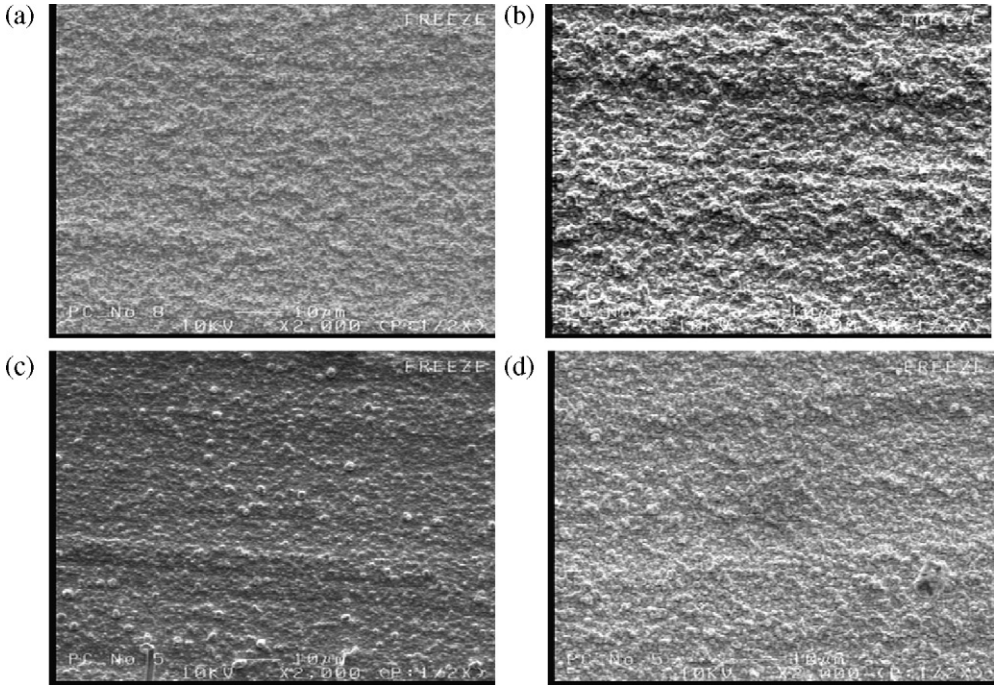

Fig. 1. SEM images of Sn–Co alloy films obtained in the plating baths with (a) 5.8, (b) 8.7, (c) 11.6, and (d) 17.3 $g\,L^{-1}$ $CoCl_2$.

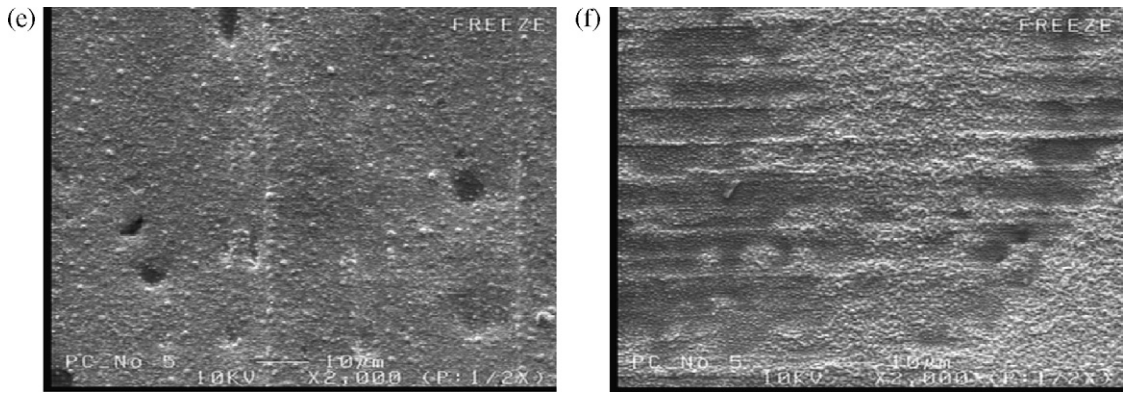

Fig. 3. SEM images of Sn–Co alloy films obtained in the plating baths with (e) 250 and (f) 350 g L^{-1} $Na_2C_4H_4O_6{\cdot}2H_2O$.

When the Pt counter electrode is used, the Co content of the film increases because the supply of Sn resource is limited from the counter electrode. Therefore, the composition is controllable by the choice of counter electrode. The electroplated films were rinsed with distilled water and then dried in a vacuum for one night.

The three-terminal swagelok-based test cell [18] was built with an alloy film, which was cut out with a round punch into a diameter of 12 mm as a working electrode. Metallic Li with a diameter of 12 mm was used as a counter electrode. Metallic Li with a diameter of 2 mm was also used as a reference electrode which was placed close by the working electrode. A solution of EC and DEC (3:7 in volume) including 1.0 mol dm^{-3} $LiPF_6$ was used as an electrolyte. A polypropylene porous membrane with a diameter of 13 mm was used as a separator.

The cell was charged at 0.1 mA cm^{-2} to 0.02 V vs. Li/Li^+ and then discharged at the same current density to 1.50 V vs. Li/Li^+ for 20 cycles. The alloy composition was verified by using X-ray fluorescence analysis (XRF). Scanning electron microscope (SEM) observation was carried out at 2000-fold magnification to investigate the film surface morphology.

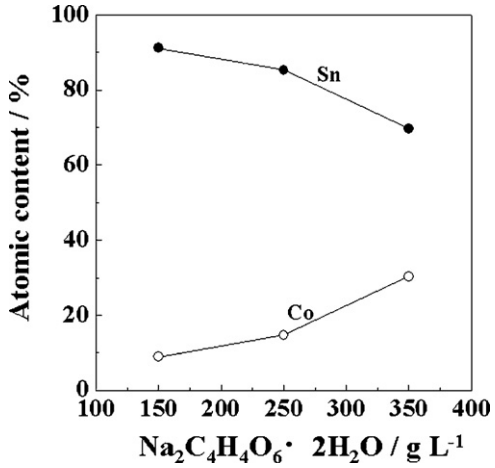

Fig. 4. Change in composition of Sn–Co alloy film as a function of $Na_2C_4H_4O_6{\cdot}2H_2O$ content in the plating bath.

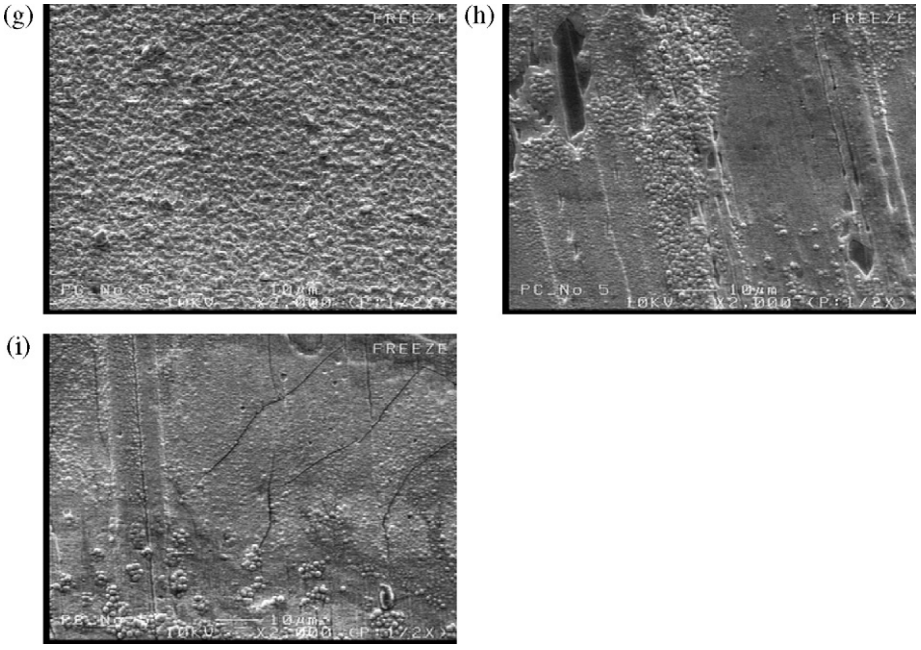

Fig. 5. SEM images of Sn–Co alloy films obtained in the plating baths with (g) 40, (h) 80, and (i) 160 g L^{-1} $K_3C_6H_5O_7{\cdot}H_2O$.

3. Results and discussion

3.1. Binary Sn–Co alloy film

SEM images of the films obtained under the bath conditions (a)–(d) are shown in Fig. 1. Some particles ranging from 0.5 to 1.5 μm were confirmed on the surface of all films. As the $CoCl_2$ content increases from 5.8 g L^{-1} to 8.7, 11.6, and 17.3 g L^{-1} in the plating bath, the particle size of the film seems to become larger. However, a surface morphology was wholly homogeneous in all cases with different amounts of $CoCl_2$. Moreover, the composition was found to be stabilized at around 92.3% Sn and 7.7% Co even though the $CoCl_2$ content increased in the plating bath as shown in Fig. 2. This fact means that there is less influence of $CoCl_2$ content on the composition under the condition of the constant complex reagent content in the plating bath.

The effect of $Na_2C_4H_4O_6{\cdot}2H_2O$ and $K_3C_6H_5O_7{\cdot}H_2O$ contents was also investigated for plating baths to prepare Sn–Co alloy film. As the amount of $Na_2C_4H_4O_6{\cdot}2H_2O$ increased from 150 g L^{-1} to 250 and 350 g L^{-1} with constant $K_3C_6H_5O_7{\cdot}H_2O$ content of 20 g L^{-1}, the film morphology changed more inhomogeneously as shown in Figs. 1(d) and 3. However, the Co content in the Sn–Co alloy film increased as the amount of the complex reagent increased as shown in Fig. 4. It is suggested that $C_4H_4O_6$ anion strongly forms the complex with Co cation by the chelate effect to reduce the difference of the standard electrode potentials. On the other hand, in the case of different $K_3C_6H_5O_7{\cdot}H_2O$ contents of 20, 40, 80, and 160 g L^{-1} with constant $Na_2C_4H_4O_6{\cdot}2H_2O$ content of 350 g L^{-1}, film surface morphology remains inhomogeneous including some cracks and incomplete coverage as shown in Figs. 3(f) and 5. In comparison with the case of $Na_2C_4H_4O_6{\cdot}2H_2O$, the composition of the film was almost stabilized in $K_3C_6H_5O_7{\cdot}H_2O$ as shown in Fig. 6. Consequently, there is less influence of $K_3C_6H_5O_7{\cdot}H_2O$ content on the composition under these conditions. However, in the case that no $K_3C_6H_5O_7{\cdot}H_2O$ was added to the plating bath, white precipitates formed. Therefore, $K_3C_6H_5O_7{\cdot}H_2O$ is a necessity for the stability of the solution.

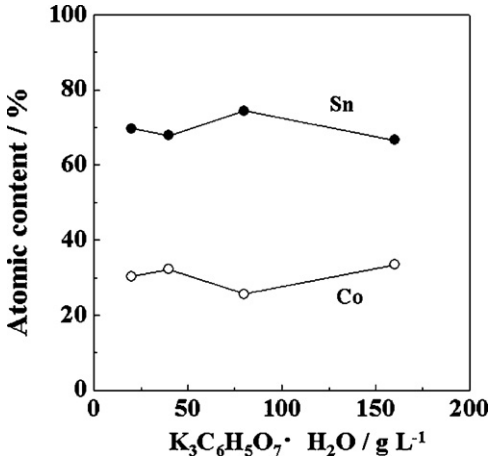

Fig. 6. Change in composition of Sn–Co alloy film as a function of $K_3C_6H_5O_7{\cdot}H_2O$ content in the plating bath.

Sn–Co alloy film with a composition of 83.3% Sn and 16.7% Co was obtained by using a Pt counter electrode instead of Sn under a bath condition (d). Co content of Sn–Co film increased from 8.9% as shown in Fig. 2 to 16.7% by using a Pt counter electrode. Thus, the choice of counter electrode is also able to control the film composition. In addition, the Sn–Co alloy film with a composition of 83.3% Sn and 16.7% Co was found to be amorphous by means of X-ray diffractometer (XRD).

3.2. Ternary Sn–Sb–Co alloy film

In order to make ternary Sn–Sb–Co alloy film, the plating baths were investigated on the basis of condition (d), which led to homogeneous Sn–Co alloy film. $SbCl_3$ was added to the bath in order to prepare Sn–Sb–Co alloy film. Fig. 7 indicates SEM images of Sn–Sb–Co alloy film obtained in the plating baths with different amounts of $SbCl_3$. In the case of 0.9 g L^{-1} $SbCl_3$, the film was homo-

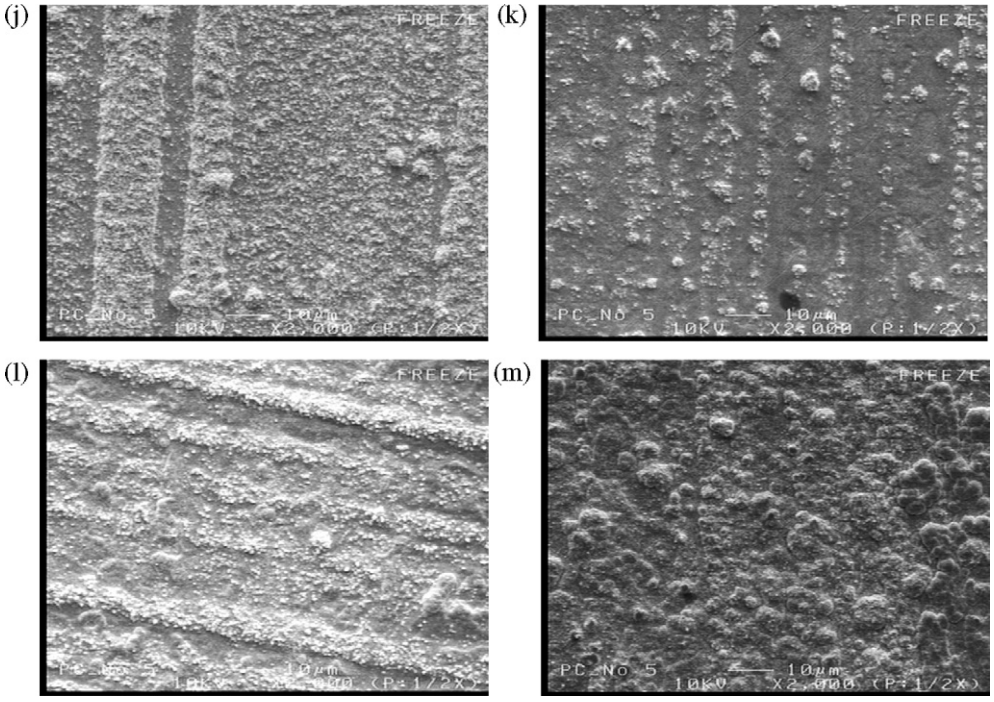

Fig. 7. SEM images of Sn–Sb–Co alloy films obtained in the plating baths with (j) 0.9, (k) 1.8, (l) 2.7, and (m) 3.6 g L^{-1} $SbCl_3$.

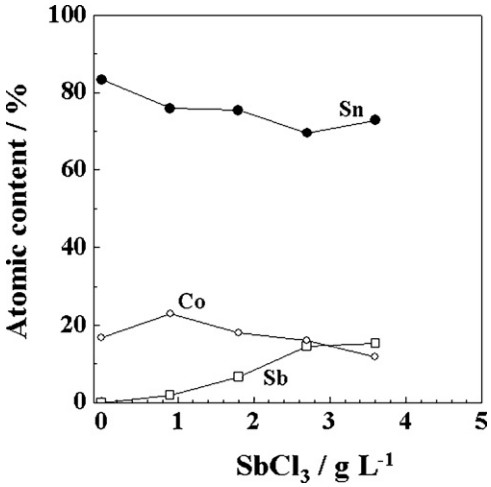

Fig. 8. Change in composition of Sn–Sb–Co alloy film as a function of $SbCl_3$ content in the plating bath.

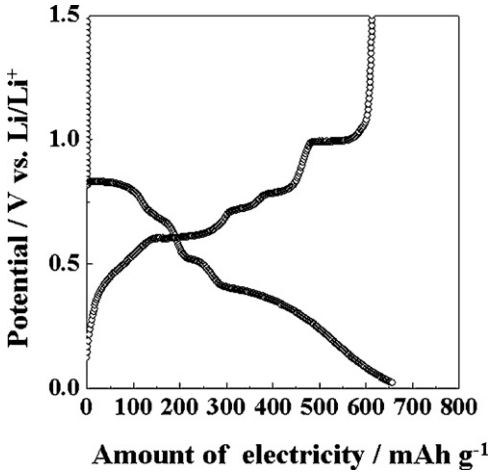

Fig. 10. Charge and discharge characteristics of Sn–Sb film electrode with a composition of 81.6% Sn and 18.4% Sb.

geneous with some particles and agglomerates on the surface. The composition was confirmed to be 75.6% Sn, 1.8% Sb, and 22.6% Co. Therefore, it was turned out that ternary Sn–Sb–Co alloy film is able to be prepared under the bath condition (j). The particles on the surface of the Sn–Sb–Co alloy film seem to decrease somewhat as the $SbCl_3$ content increases from 0.9 to 1.8 g L^{-1} in the bath. The change in the composition of Sn–Sb–Co alloy film is shown in Fig. 8. The Sb content in Sn–Sb–Co alloy film was found to increase as the amount of $SbCl_3$ increases in the plating bath. This result means the ternary Sn–Sb–Co is able to be prepared under the bath conditions (k)–(m) as well as (j). In addition, the Sn–Sb–Co alloy film obtained in the bath (k), which is a composition of 75.4% Sn, 6.5% Sb, and 18.1% Co, was found to include SnSb, $CoSn_2$, and Sn phase by XRD analysis.

3.3. Electrochemical performance of Sn–Co and Sn–Sb–Co film electrodes

Fig. 9 shows charge and discharge characteristics of Sn–Co alloy film electrode with a composition of 83.3% Sn and 16.7% Co. The amount of initial charging electricity and the discharge capacity were 743 and 561 mAh g^{-1}, respectively. Namely, the discharge to charge efficiency is calculated to 75.6%. The Sn–Co alloy film electrode showed low potential plateau at around 0.32 V vs. Li/Li^+ in the first charging process. On the other hand, two potential plateaus at around 0.45 and 0.6 V vs. Li/Li^+ were able to be confirmed in the discharging process. The charge-discharge curves of Sn–Co alloy film electrode are quite different from Sn–Sb film electrode with a composition of 81.6% Sn and 18.4% Sb as shown in Fig. 10. The Sn–Sb alloy film electrode showed a larger discharge capacity of 614 mAh g^{-1} and distinct four potential plateaus in the charge-discharge processes. It has been reported that Li_3Sb is formed at the first potential plateau and then Sn domain reacts with Li for Li–Sn alloy formation, i.e. Li_2Sn_5, LiSn, and Li_7Sn_3 at subsequent plateaus of 0.7, 0.6, and 0.4 V vs. Li/Li^+, respectively in the charging process [3]. Below the fourth potential plateau of 0.4 V vs. Li/Li^+, Li insertion further proceeds to form $Li_{22}Sn_5$. It can be presumed that the delivered capacity of Sn–Sb film electrode is smaller than theoretical capacity due to a kinetic problem.

Fig. 11 indicates charge and discharge characteristics of Sn–Sb–Co alloy film electrode with a composition of 75.4% Sn, 6.5% Sb, and 18.1% Co. The amount of initial charging electricity and discharge capacity were 496 and 380 mAh g^{-1}, respectively, which means the efficiency of 76.6%. The charge and discharge characteristics are similar to electroplated Sn electrode as shown in previous reported [2].

Fig. 12 shows cycle performance of Sn–Sb–Co, Sn–Co, and Sn–Sb alloy film electrodes. The Sn–Sb alloy film electrode showed the largest initial discharge capacity among them. However, the capac-

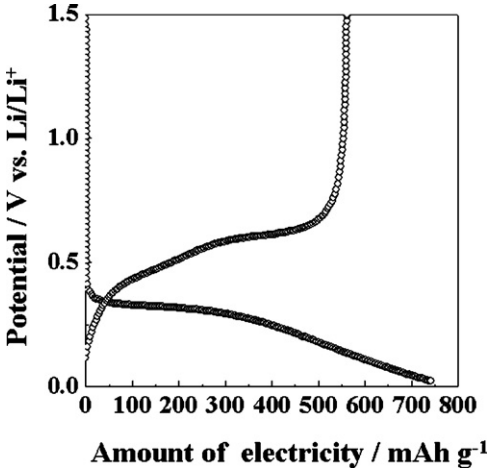

Fig. 9. Charge and discharge characteristics of Sn–Co film electrode with a composition of 83.3% Sn and 16.7% Co.

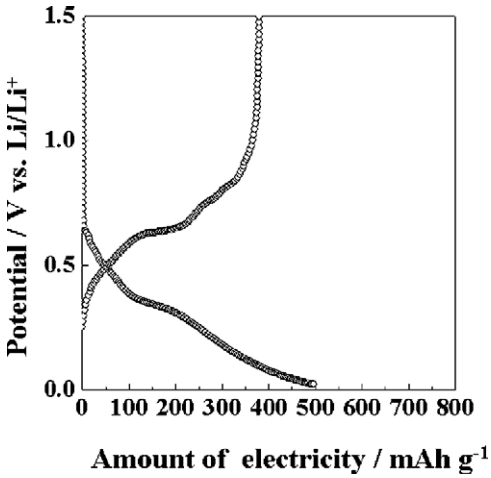

Fig. 11. Charge and discharge characteristics of Sn–Sb–Co film electrode with a composition of 75.4% Sn, 6.5% Sb, and 18.1% Co.

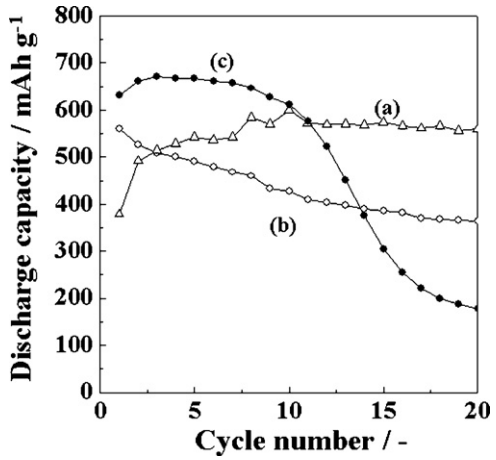

Fig. 12. Cycle performances of (a) Sn–Sb–Co, (b) Sn–Co, and (c) Sn–Sb film electrodes.

ity drastically decreased after the 10th cycle. The Sn–Co alloy film electrode gave better cycleability since the volume change reduces by inactive Co matrix during cycling [9]. Compared with Sn–Sb and Sn–Co alloys, the capacity of the Sn–Sb–Co film electrode gradually increased from the 1st to the 10th cycle and was then stabilized around 580 mAh g^{-1} at subsequent cycles. The reason can be considered as follows. Li_3Sb is first formed around Sn domain from SnSb phase, which can reduce the volume change of following Li-insertion into Sn in the charging process. As the cycle proceeds, Sn tends to aggregate resulting in significant volume change and capacity decay. However, inactive Co matrix leads to prevent the aggregation with cycling. As a result, the Sn–Sb–Co alloy film electrode gave much better cycleability compared with Sn–Sb and Sn–Co electrodes.

4. Conclusions

Ternary Sn–Sb–Co alloy film was successfully prepared using a plating bath with $SnCl_2{\cdot}2H_2O$, $CoCl_2$, $SbCl_3$, $Na_2C_4H_4O_6{\cdot}2H_2O$, $K_3C_6H_5O_7{\cdot}H_2O$, and gelatine. The Sb content in Sn–Sb–Co alloy film was found to increase as the amount of $SbCl_3$ increased in the plating bath. This result means the composition of ternary Sn–Sb–Co can be controllable by the amount of $SbCl_3$. The initial charging electricity and discharge capacity of Sn–Sb–Co alloy film electrode with a composition of 75.4% Sn, 6.5% Sb, and 18.1% Co were 496 and 380 mAh g^{-1}, respectively. The capacity of the Sn–Sb–Co alloy film electrode gradually increased from the 1st to the 10th cycle and was then stabilized around 580 mAh g^{-1} at subsequent cycles. Furthermore, the Sn–Sb–Co alloy film electrode was found to give much better cycle performance compared to binary Sn–Co and Sn–Sb alloys. Therefore, ternary Sn–Sb–Co alloy is a promising candidate for a large-capacity negative active material.

Binary Sn–Co alloy film was also successfully prepared using a plating bath with $SnCl_2{\cdot}2H_2O$, $CoCl_2$, $Na_2C_4H_4O_6{\cdot}2H_2O$, $K_3C_6H_5O_7{\cdot}H_2O$, and gelatine. The addition of $Na_2C_4H_4O_6{\cdot}2H_2O$ was found to strongly influence the morphology and composition of Sn–Co film. It is suggested that $C_4H_4O_6$ anion strongly forms the complex with Co cation by the chelate effect to reduce the difference of the standard electrode potentials. As a result, the film morphology and composition can be controlled by the $Na_2C_4H_4O_6{\cdot}2H_2O$ contents in the plating bath.

References

[1] J.O. Besenhard, J. Yang, M. Winter, Journal of Power Sources 68 (1997) 87.
[2] M. Winter, J.O. Besenhard, Electrochimica Acta 45 (1999) 31.
[3] C.J. Wen, R.A. Huggins, Journal of The Electrochemical Society 128 (1981) 1181.
[4] J. Yang, M. Winter, J.O. Besenhard, Solid State Ionics 90 (1996) 281.
[5] J.O. Besenhard, M. Wachtler, M. Winter, R. Andreaus, I. Rom, W. Sitte, Journal of Power Sources 81/82 (1999) 268.
[6] J. Yang, Y. Takeda, Q. Li, N. Imanishi, O. Yamamoto, Journal of Power Sources 90 (2000) 64.
[7] M. Wachtler, M.R. Wagner, M. Schmied, M. Winter, J.O. Besenhard, Journal of Electroanalytical Chemistry 510 (2001) 12.
[8] M. Wachtler, J.O. Besenhard, M. Winter, Journal of Power Sources 94 (2001) 189.
[9] M. Wachtler, M. Winter, J.O. Besenhard, Journal of Power Sources 105 (2002) 151.
[10] H. Mukaibo, T. Osaka, P. Reale, S. Panero, B. Scrosati, M. Wachtler, Journal of Power Sources 132 (2004) 225.
[11] A. Trifonova, M. Wachtler, M.R. Wagner, H. Schroettner, C. Mitterbauer, F. Hofer, K.-C. Moeller, M. Winter, J.O. Besenhard, Solid State Ionics 168 (2004) 51.
[12] S.A. Needham, G.X. Wang, H.K. Liu, Journal of Alloys and Compounds 400 (2005) 234.
[13] E. Gomez, E. Guaus, J. Torrent, X. Alcobe, E. Valles, Journal of Applied Electrochemistry 31 (2001) 349.
[14] N. Tamura, M. Fujimoto, M. Kamino, S. Fujitani, Electrochimica Acta 49 (2004) 1949.
[15] N. Tamura, Y. Kato, A. Mikami, M. Kamino, S. Matsuta, S. Fujitani, Journal of The Electrochemical Society 153 (2006) A1626.
[16] N. Tamura, Y. Kato, A. Mikami, M. Kamino, S. Matsuta, S. Fujitani, Journal of The Electrochemical Society 153 (2006) A2227.
[17] F.-S. Ke, L. Huang, H.-B. Wei, J.-S. Cai, X.-Y. Fan, F.-Z. Yang, S.-G. Sun, Journal of Power Sources 170 (2007) 450.
[18] M. Sternad, E. Lanzer, N. Hochgatterer, S. Kollor, P. Rainmann, M. Schmuck, M. Schweiger, M. Takehara, M. Ue, M. Winter, 212th ECS Meeting, Washington, DC, 2007 (abstract 689).